Energetic Consequences of the Multidimensional Nature of Internal Rotation in Acetaldehyde†

Lionel Goodman,* Tapanendu Kundu,§ and Jerzy Leszczynski‡

Contribution from the Wright and Rieman Chemistry Laboratories, Rutgers University, New Burnswick, New Jersey 08903

Received July 11, 1994⊗

Abstract: Ab initio calculations are reported which partition the energetics of internal rotation for ground state acetaldehyde according to potential type (repulsive and attractive), symmetry (σ and π), region (atomic basin), and nuclear virial (rotational path). We conclude that the origin of the barrier is complex, involving interplay of kinetic and potential energies of π and σ electrons. The formation of the barrier can be divided into three conceptual steps. (1) Rigid rotation occurs where the skeleton is frozen at the eclipsed equilibrium geometry during methyl rotation. This first step frequently leads to reasonable barrier heights, but it engenders increased kinetic energy of the π electrons. (2) To relieve the repulsive π-nuclear virial, the molecule relaxes by C−C bond lengthening. This lengthening causes both σ and π core energies to increase. But the greater sensitivity of σ electrons to C−C bond lengthening overwhlems the π contribution. (3) Other skeletal and methyl flexings, necessary to achieve the fully relaxed barrier top, correct the energetics governing (1) + (2). The outcome of all three steps is that changes in σ orbitals through an increase in σ nuclear−electron attraction energy contribute to the fully relaxed barrier. The π-fragment model for internal rotation energetics considers just the first step, which neglects skeletal flexing.

Introduction

Much of the recent spelunking into torsional potential barrier heights and shapes has resulted from (1) the ability of large scale ab initio computations to accurately predict overall molecular geometries which include the skeletal flexing that takes place as internal rotation proceeds and (2) the ability of high-resolution FTIR, microwave, and jet electronic spectroscopies to obtain precise torsional fundamental and overtone frequencies—leading to accurate torsional potential shape information. Acetaldehyde, one of the simplest conjugated molecules capable of internal rotation (see Figure 1), has had almost as much attention as ethane (barrier ~1000 cm^{-1}), long regarded as a key molecule in understanding the energetics of internal rotation barriers.

Early (late sixties) ideas on the ethane barrier invoked Pauli-like exchange repulsions between C−H bond orbitals[1] (an excellent review is given by R. M. Pitzer[2]). But even for this very well studied molecule the cause for the barrier is not settled. Bader, Chessman, Ladig, Wiberg, and Breneman[3] (BCLWB) have recently offered a provocative alternate explanation for the barrier in terms of the polarization of charge density in the C−C bond. BCLWB rationalize the ethane barrier arising from transformation of the molecular S_3 symmetry in the equilibrium conformation to C_3 at the top of the barrier. They argue that symmetry reduction induces quadrupole polarization in the electron cloud. Because this type of charge distribution is less effective in binding the carbon nuclei it causes lengthening of the bond with concomitant reduction in the attractive electron−nuclear interactions, which overwhelm an accompanying weaker reduction in the repulsive energies.

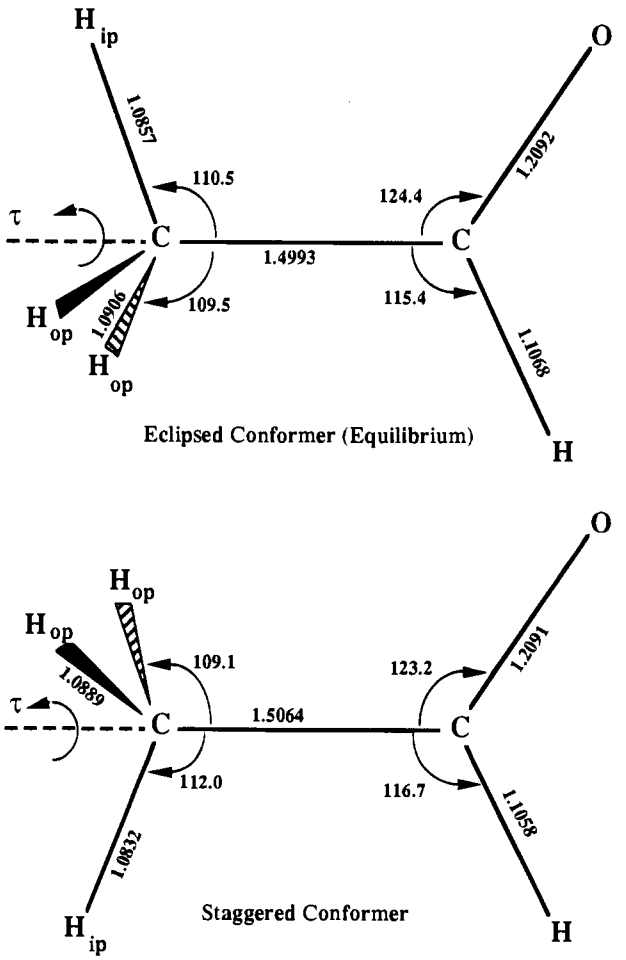

Figure 1. MP2/6-311G(3df,2p) optimized geometries for acetaldehyde equilibrium eclipsed (E) and top-of-barrier staggered (S) conformers.

There have been many microwave and infrared studies on acetaldehyde culminating in the high-resolution experiments of Belov et al.[4] and Kleiner et al.[5] accurately fixing both the barrier

* To whom correspondence should be addressed.

† Supported by Petroleum Research and National Science Foundations.

§ Present address: Physics Department, Indian Institute of Technology, Powai, Bombay 400076, India.

‡ Permanent Address: Chemistry Department, Jackson State University, Jackson, Mississipi 39217-0510.

⊗ Abstract published in *Advance ACS Abstracts,* February 1, 1995.

(1) Sovers, O. J.; Kern, C. W.; Pitzer, R. M.; Karplus, M. *J. Chem. Phys.* **1968**, *49*, 2592.

(2) Pitzer, R. M. *Acc. Chem. Res.* **1983**, *16*, 207.

(3) Bader, R. F. W.; Chessman, J. R.; Laidig, K. E.; Wiberg, K. B.; Breneman, C. *J. Am. Chem. Soc.* **1990**, *112*, 6530.

0002-7863/95/1517-2082$09.00/0

(at 408 cm^{-1}) and flattened shape ($V_6 < 0$) of the potential for 180° internal rotation to the staggered conformer. Thus the acetaldehyde barrier approximates one-third that in ethane. These facts would appear to fit the Pauli repulsion model since there is one CH−CH eclipsed interaction at acetaldehyde's metastable geometry (Figure 1). In ethane there are three.

In the early seventies Davidson and Allen[6] took another tack. From a Slater-type orbital calculation they concluded that the barrier is attractive dominant, i.e., it mainly arises from reduction of attractive electron−nuclear interactions. Several years later Hehre, Pople, and Devaquet[7] (HPD), using higher order split valence shell level molecular orbital theory, proposed that it is the π interactions that dominate. Ignoring repulsive and attractive interactions within the σ framework, their model has the barrier arising from two effects: (1) *increased repulsion* between filled methyl group π-like fragment orbitals (π_{Me}) and filled π-orbitals in the C=O double bond ($\pi_{C=O}$) [this repulsion is greater for the staggered conformation] and (2) *decreased attraction* between HOMO and LUMO π-fragment orbitals in the staggered conformation. Both of these interactions ($\pi_{Me}-\pi_{C=O}^*$ and $\pi_{Me}^*-\pi_{C=O}$) are stabilizing because they involve only two electrons as opposed to the 4-electron repulsions arising from the filled π-fragment orbitals in (1). The HPD model has been extended to acetaldehyde lowest energy radical cations, anions, and triplet states by Dorigo, Pratt, and Houk[8] taking into account different orbital occupancies along with $\pi_{Me}^*-\pi_{C=O}^*$ interactions which are absent in the ground state of the neutral molecule. Their barrier prediction for the π-cation is less than half that of the ground state contrary to that obtained from Pauli repulsion considerations.

While the focus of the π-fragment model has been on the barrier *height* (difference between staggered and eclipsed conformation energies), it is clear that the most significant information can be obtained by concentrating on individual (potential and kinetic) energy components.[9] This is because the small total energy change associated with internal rotation (generally in the 10^2 and 10^3 cm^{-1} range) is nearly always very much smaller than the separate potential energy terms. Thus it is possible for a model to give reasonable rotation barriers even though it incorrectly predicts the sense of attractive and repulsive potential energy changes.

The most primitive approach to internal rotation in a single rotor molecule like acetaldehyde is a one-dimensional (i.e., rigid rotation) model comprising only the torsional coordinate. By this simple model, ab initio predicted barriers are only ~10% above the experimental barrier (see Table 1). Ozkabak and Goodman,[10] arguing that internal rotation is a multidimensional process, addressed the skeletal flexing accompanying rotation. A major conclusion was that lengthening of the C−C bond in acetaldehyde (Figure 1) is an important factor for barrier determination. Subsequent studies[11] showed that the key to the potential shape near the bottom of the well is provided by aldehyde-hydrogen flexing. The important deduction of the flexing studies is that the flattened shape and narrow barrier in acetaldehyde cannot be understood without concomitant out-of-plane wagging of the aldehyde-hydrogen and the methyl-group torsion. Thus our present picture of internal rotation in acetaldehyde is that of a highly impure vibration comprising large-amplitude torsion coupled to skeletal normal modes.

Table 1. 6-311G(3df,2p) ab Initio Acetaldehyde Torsional Barriers and Important Vibrational Energy Changes (cm^{-1})

Barriers	ΔE^a	ΔE^b
adjusted experiment[c]	416	
ST4CCD/6-311G(3df,2p)	415[d]	463
MP4(STDQ)/6-311G(3df,2p)	412[d]	455
MP2/6-311G(3df,2p)	438[d]	475
HF/6-311G(3df,2p)	463[d]	519
vib freq changes		$\Delta\omega^e$
ν_8 a′ C−C stretch		−32
ν_9 a′ C−C−H aldehyde bend		+44
ν_{14} a″ C−C=O wag		−22
ν_{13} a″ asymmetric methyl C−H stretch		+19

[a] Electronic energy difference between separately optimized staggered (S) and eclipsed (E) conformers. [b] Rigid rotation calculation, i.e., E ⟶ S[RF]. See text. [c] The 408 cm^{-1} measured barrier (ref 4) has been adjusted by subtracting an estimated −8 cm^{-1} zero-point energy difference between staggered and eclipsed conformers. [d] Reference 12. [e] Staggered − elipsed conformation harmonic vibrational frequency difference calculated by following the procedure in ref 16.

When this multidimensional picture for internal rotation in acetaldehyde is combined with an accurate treatment of electron correlation,[12] the outcome is a quantitatively accurate barrier (see Table 1). The small correction (40−50 cm^{-1}) to the barrier calculated by the rigid rotation model leads to the delusion that the barrier can be understood in terms of rigid rotation. We will show that useful generalizations have not arisen from this approach because the multidimensional corrections to individual repulsions and attractions are very large and in fact change the signs of the individual energy components. Ab initio calculations of electronic properties of small molecules have frequently stressed the need for a large balanced basis set, a point that needs emphasis since internal rotation barriers are electronic, resulting from cancellations between repulsions and attractions. In this paper we discuss acetaldehyde barrier energetics using a 6-311G(3df,2p)-triple valence-ζ basis set augmented by extensive polarization. In addition, validating calculations are made at the modest 6-31G(d,p) and diffuse function containing 6-311+G(3df,2p) bases. Since the simple π-fragment ideas by HPD seem to account for many of the key experimental observations on small conjugated methyl molecules, we pay particular attention to validating this model. In our discussion we have been influenced by Allen's ideas on energy partitioning.[6]

Calculations

To understand the physics of acetaldehyde hindered rotation we carried out interlocking calculations designed to focus on both spatial region and interaction type, employing three approaches. The first partitions the various *overall* energy terms contributing to the eclipsed (E) ⟶ staggered (S) barrier, i.e. the differences in attractive electron−nuclear energy (ΔV_{ne}), as well as differences in the repulsive energies: kinetic (ΔT), nuclear−nuclear (ΔV_{nn}), and electron−electron (ΔV_{ee}). These partitioned energy calculations were made at frozen core 2nd order Møller−Plesset perturbation theory (MP2) and Hartree−Fock (HF) levels using three basis sets. The first is the 6-311G(3df,2p) basis set that we previously found had converged in the calculation of barrier height. Because it is important in energy partitioning that virials are

(4) Belov, S. P.; Tretyakov, M. Yu.; Kleiner, I.; Hougen, J. T. *J. Mol. Spectrosc.* **1993**, *160*, 61.
(5) (a) Kleiner, I.; Hougen, J. T.; Suenram, R. D.; Lovas, F. J.; Godefroid, M. *J. Mol. Spectrosc.* **1991**, *148*, 38. (b) Kleiner, I.; Hougen, J. T.; Suenram, R. D.; Lovas, F. J. *J. Mol. Spectrosc.* **1992**, *153*, 578.
(6) Davidson, R. B.; Allen, L. C. *J. Chem. Phys.* **1971**, *55*, 519.
(7) Hehre, W. J.; Pople, J. A.; Devaquet, A. J. P. *J. Am. Chem. Soc.* **1976**, *98*, 664.
(8) Dorigo, A. E.; Pratt, D. W.; Houk, K. N. *J. Am. Chem. Soc.* **1987**, *109*, 6591.
(9) (a) Allen, L. C. *Chem. Phys. Lett* **1968**, *2*, 597. (b) Payne, P. W.; Allen, L. C. *Applications of Electronic Structure Theory*; Schaefer, H. F., Ed.; Plenum: New York, 1977; pp 29−108.
(10) Ozkabak, A. G.; Goodman, L. *J. Chem. Phys.* **1992**, *96*, 5958.
(11) (a) Goodman, L.; Leszczynski, J.; Kundu, T. *J. Chem. Phys.* **1994**, *100*, 1274. (b) Nino, A.; Munoz-caro, C.; Moule, D. C. *J. Phys. Chem.* **1994**, *98*, 1519.
(12) Leszczynski, J.; Goodman, L. *J. Chem. Phys.* **1994**, *99*, 4867.

satisfied we also checked these calculations against two other basis sets, 6-311+G(3df,2p) and 6-31G(d,p), which satisfy the virial theorem more precisely than the former (see the next section).

Software limitations did not allow us to go beyond the MP2 level to obtain partitioned energy terms. Since MP2 calculations are not variational, MP2 partitioned energies are not on the same footing as HF. Although this is not believed to lead to significant errors, we always compare MP2 and HF partitioned energies to make sure there is sign consistency. The calculations in this approach were carried out taking different internal rotation paths through various virtual states to reach the staggered conformation. These virtual states are discussed in section II.3 of the Results and Discussion.

These overall energy calculations were carried out using the GAUSSIAN 92 suite of programs[13] on a Cray C-90 processor at the Pittsburgh Supercomputer Center. Default geometry optimization thresholds (checked with tight options) were as previously described.[10] Single-point calculations were carried out at the MP2 optimized geometries, except for the virtual states discussed in the next section.

The second set of calculations, yielding σ and π separation[14] of kinetic and core energies, were carried out again using GAUSSIAN 92 software, but in this case modified to achieve symmetry separation of energy terms. These calculations were performed on the Hewlett-Packard 9000/735 processor in the High Performance Computation Project of the Rutgers University Chemistry Department.

The third approach focuses on the spatial regions of the interactions by making use of space partitioning into atomic basins as developed by Bader.[15] The Bader scheme partitions the molecular space into distinct nonoverlapping regions (atomic basins) with each region containing a single atom. The staggered−eclipsed difference for the various attractive and repulsive interactions can then be calculated for local basins around each atom. These calculations employed SADDLE[16] to obtain the 12 acetaldehyde bond critical points and finally PROAIM[15] to obtain the local basin energies. They were carried out on the Silicon Graphics IRIX R3000 processor in the Rutgers Chemistry Department. The local basin computations were regarded as converged when the difference in atomic basin G and K kinetic energies[16] was $\leq 1 \times 10^{-5}$ hartree except for the aldehyde carbon where the difference was $\leq 1 \times 10^{-4}$ hartree.

Results and Discussion

I. Barrier Energy. The skeletal flexing which accompanies torsional rotation of the methyl group implies changes in the normal modes of the molecule, even those which do not involve methyl torsional motion, per se. In terms of the Born−Oppenheimer approximation, account of these changes can be obtained by considering the alteration in zero-point energy of all the "other" normal modes (i.e., those not including the methyl torsional vibration). Accordingly an effective barrier energy, $\Delta E_{\text{barrier}}$, can be written

$$\Delta E_{\text{barrier}} = \Delta E + \Delta(\text{ZPE}) \qquad (1)$$

In eq 1 ΔE is the ab initio calculated electronic energy difference between the acetaldehyde global minimum staggered (S) and eclipsed (E) conformers. The term Δ(ZPE) is the zero-point energy difference taken between these two conformers, summed over the 14 high-frequency modes (i.e., torsion not included). It is $\Delta E_{\text{barrier}}$ that is usually reported in microwave analysis.

We estimate Δ(ZPE) by scaling MP2/6-311G(3df,2p) ab initio harmonic force constants[17] to fit the experimental eclipsed conformer frequencies using separate scaling factors for diagonal and off-diagonal force constants. These scaling factors are carried over to the staggered conformer. We have shown elsewhere that this theory level reproduces the 14 acetaldehyde anharmonicity-corrected experimental high-energy normal mode frequencies and deuterium shifts for the stable eclipsed conformer with an rms error of 4.3 cm^{-1}.[17] The largest predicted frequency change, >40 cm^{-1} increase on going to the staggered conformer, occurs for the a′ in-plane CCH aldehyde bending mode, ν_9 observed at 866 cm^{-1} in gaseous acetaldehyde. Significant decreases are also found for the C−C stretching mode, ν_8 observed at 1114 cm^{-1}, and for the C−C=O out-of-plane wagging mode, ν_{14} observed at 764 cm^{-1} (Table 1). The predicted harmonic contribution to Δ(ZPE) is −8.2 cm^{-1}.

Thus we estimate the harmonic contribution to the zero-point energy term to be in the vicinity of −8 cm^{-1}. It is somewhat smaller than the −16 to −19 cm^{-1} correction predicted by Bell[18] in his thorough study of acetaldehyde vibrational constants by purely ab initio HF/6-31G and MP2/6-31 G(d,p) calculations. Although anharmonicities have not been included, these relatively small harmonic Δ(ZPE) values, 2−4% of the measured barrier, estimated by different approaches, indicate that unlike for ethane[19] the microwave reported acetaldehyde barrier is largely electronic in nature.

Table 2. Energy Terms for Fully Relaxed Internal Rotation in Acetaldehyde (cm^{-1})

energy diff[a]	MP2[b]	MP2[c]	HF[d]
total energy, ΔE	438	402	373
kinetic energy, ΔT	−176	−328	−366
potential energy, ΔV	614	730	739
nuclear−nuclear repulsion energy, ΔV_{nn}	−5822	−3716	−4431
electron−electron repulsion energy, ΔV_{ee}	−3313	−1921	−692
nuclear−electron attraction energy, ΔV_{ne}	9749	6367	5862
repulsive energy, $\Delta V_r = \Delta V_{ee} + \Delta V_{nn}$	−9135	−5637	−5123
electronic potential energy, $\Delta V_e = \Delta V_{ee} + \Delta V_{ne}$	6436	4446	5170

[a] Difference between staggered (180°) and equilibrium eclipsed (0°) conformers (Figure 1). Positive energy differences are destabilizing (barrier forming) and negative differences are stabilizing (barrier reducing). [b] Calculations are at the MP2/6-311G(3df,2p) fully optimized eclipsed and staggered geometries. [c] As in footnote *b* except the basis set is 6-311+G(3df,2p). [d] HF for the 6-31G(d,p) basis set.

II. Energy Partitioning. (a) Overall. 1. Fully Relaxed Internal Rotation (E ⟶ S). We first consider overall partitioning of the total electronic energy change

$$\Delta E = \Delta T + \Delta V_{ee} + \Delta V_{nn} + \Delta V_{ne} \qquad (2)$$

during methyl group torsional rotation from the equilibrium eclipsed position to the top-of-the-barrier staggered position (Figure 1). The attractive and repulsive contributions to the total energy change are $\Delta V_a \equiv \Delta V_{ne}$ and $\Delta T + \Delta V_r$, respectively ($\Delta V_r \equiv \Delta V_{ee} + \Delta V_{nn}$). It is also useful to define the electronic potential $\Delta V_e \equiv \Delta V_{ee} + \Delta V_{ne}$.

In this calculation the molecular geometry is fully optimized during methyl-group rotation. The quantity of interest is the difference between the individual energy terms for staggered and eclipsed conformations. The results are given in Table 2 for three levels, MP2/6-311G(3df,2p), MP2/6-311+G(3df,2p), and HF/6-31G(d,p). All three single-point calculations are carried out at the appropriate optimized geometries. We note that the virial theorem, $\Delta E = -\Delta T$, is not satisfied for the MP2 calculations for the 6-311G(3df,2p) basis set, since $\Delta E + \Delta T$

(13) Frisch, M. J.; Head-Gordon, M.; Trucks, G. W.; Foresman, J. B.; Schlegel, H. B.; Raghavachari, K.; Robb, M.; Binkley, J. S.; Gonzalez, C.; Defrees, D. J.; Fox, D. J.; Whiteside, R. A.; Seeger, R.; Melius, C. F.; Baker, J.; Martin, R. L.; Kahn, L. R.; Stewart, J. J. P.; Topiol, S.; Pople, J. A. GAUSSIAN 92; Gaussian Inc.: Pittsburgh, PA, 1992.

(14) C_s symmetry, non-nodal a′ orbitals represent σ-type and nodal a″ ones represent π-type.

(15) Bader, R. F. W. *Acc. Chem. Res.* **1985**, *18*, 9.

(16) Biegler-Konig, F. W.; Bader, R. F. W.; Tang, T. H. *J. Comp. Chem.* **1982**, *3*, 317.

(17) Wiberg, K. B.; Thiel, Y.; Goodman, L.; Leszczynski, J. *J. Phys. Chem.*, in press.

(18) Bell, S. *J. Mol. Struct.* **1994**, *320*, 125.

(19) Kirtman, B.; Palke, W. E.; Ewig, C. S. *J. Chem. Phys.* **1976**, *64*, 1883.

> 250 cm^{-1}, an appreciable fraction of ΔE, itself. When the basis set is expanded to include diffuse functions on the heavy atoms [MP2/6-311+G(3df,2p)], there is improvement in virial theorem satisfaction, $\Delta E + \Delta T < 80$ cm^{-1} (Table 2). The variational HF calculation well satisfies the virial theorem, $\Delta E + \Delta T < 7$ cm^{-1}, despite the modest basis. The rational for this calculation is that the Hartree–Fock method—which even with modest basis sets predicts reasonable barriers—must correctly describe the physics that causes these barriers.

We emphasize that although there are large quantitative differences between HF and MP2 partitioned energies, all calculation levels yield the same qualitative outcome: an increase in potential energy, despite decreases in overall electron and nuclear repulsion energies on torsional rotation to the barrier top. At the same time kinetic energy decreases. Consequently repulsions, both electron and nuclear, do not represent barrier-forming energetics. Table 2 shows that the increase in energy of the staggered conformation actually results entirely from an increase in the nuclear–electron attraction energy (i.e. $\Delta V_a > 0$) and that this conclusion is independent of basis set expansion or whether correlation is included or not. In addition all calculations have the same inequalities. Hence conclusions that we draw in subsequent sections are not calculation level dependent.

There is a temptation to identify the increase in electron–nuclear attraction energy as the "origin" of the barrier. However, breakdown of the energy difference between the eclipsed and staggered geometries in terms of antagonistic ΔV and ΔT components does not, in and of itself, reveal driving forces for the energy shift. This is as true for reaction energy between reactants and products as it is for the energy barrier for internal rotation.[20] Bond formation in H_2^+ provides an illustration. An analysis of the energetics of the H_2^+ bond was carried out in a pioneering series of publications by Ruedenberg more than two decades ago.[20,21] Here $\Delta E = E(H_2^+) - E(H + H^+)$ is negative *because* $\Delta V < 0$ *in spite of* $\Delta T > 0$ (just the reverse of the energetics of acetaldehyde internal rotation). Nonetheless, Ruedenberg's in-depth analysis showed that the bond formation is a consequence of the behavior of the *kinetic energy*.[21]

2. Rigid Rotation (E ⟶ S[RF]). Rigid rotation fixes the skeleton and skeletal hydrogens at the geometry of the eclipsed conformer. The methyl-group bond lengths and internal angles are also frozen at their geometry in the eclipsed conformer, except that the hydrogen atoms are rotated by 180°. The usefulness of this process stems both from its simplicity and from its isolation of the effect of methyl rotation from other molecular structural changes that accompany rotation. It also has historical significance, since E ⟶ S[RF] (RF designates rigid frame) represents the much employed one-dimensional rigid rotation model for methyl torsion. Many of the ideas about internal rotation have stemmed from this model. The energetics for this internal rotation process is compared to the fully relaxed one in Figure 2. While the total energy change lies modestly above the true barrier, E ⟶ S (Table 3), the individual energy term changes are much more significant. Our interpretive analysis is directed toward understanding why the energy lowering between S and S[RF] occurs. We make use of our conclusion that energy partitioning at the MP2/6-311G(3df,2p) level is qualitatively sufficient to give the correct *signs*.

The energy terms given in Table 3 show that rigid torsional rotation increases the kinetic energy but decreases the potential energy (despite increases in electron and nuclear repulsion energies). This decrease results from a decrease in electron–nuclear attraction energy. Since the kinetic energy increases more strongly than the potential energy decreases, there is an overall raising of the staggered conformation energy above the eclipsed one. We emphasize that these senses are reversed from that for the fully relaxed E ⟶ S process given in Table 2. Table 3 reveals a fundamentally important relationship between fully relaxed and rigid rotation energetics: ΔT(S[RF] − S) and ΔV(S[RF] − S) are essentially interchanged. We will comment on this interchange further in sections IIb and III. As might be expected, changes in the nuclear repulsion energy depend on methyl conformational details. There are alternate ways of regarding the methyl group as it rotates. If the methyl group is regarded as a rigid C_{3v} top, nuclear repulsion decreases on torsional rotation. Allowing the methyl group to fold, as it actually does when undergoing torsion, increases the nuclear repulsion as it does for the frozen eclipsed calculation given in Table 3.

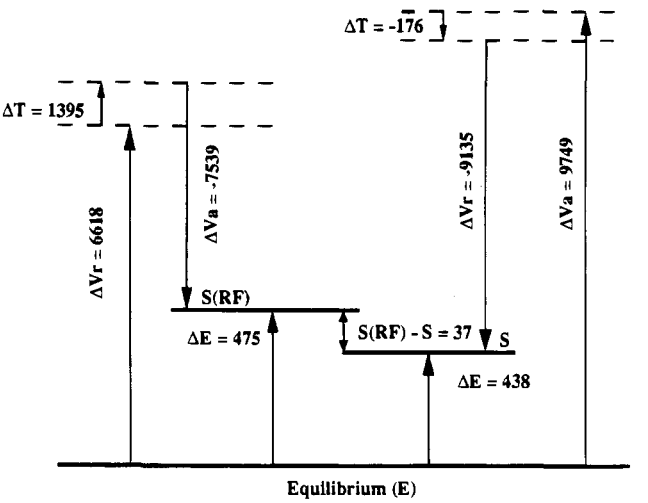

Figure 2. Comparison of energy changes (cm^{-1}) for internal rotation of the eclipsed conformer (E) into the fully relaxed staggered conformer (S) ($\tau = 180°$) and into the frozen (rigid frame) staggered conformer (S[RF]). Solid lines represent state (E, S, and S[RF]) energies; dashed lines are used to show energy partitioning and have no physical significance.

Table 3. MP2/6-311G(3df,2p) Partitioned Energy Difference for E ⟶ S[RF] and S[RF] ⟶ S (in cm^{-1})[a]

energy diff[b]	(S[RF]) − (E)	(S) − (S[RF])
ΔE	475	−37
ΔT	1395	−1571
ΔV	−920	1534
ΔV_{nn}	2771	−8593
ΔV_{ee}	3847	−7160
ΔV_{ne}	−7539	17288
ΔV_r	6618	−15753

[a] S[RF] represents rigid rotation, i.e. the molecule is fixed at the equilibrium geometry except the methyl group is rotated 180° (see text); E represents the equilibrium eclipsed conformer and S the fully relaxed staggered conformer. [b] See Table 2 footnote *a*.

3. Rotation Paths. The skeletal structural changes that accompany methyl rotation are (1) lengthening of the C–C bond and (2) narrowing of the CCO angle and concomitant widening of the CCH_{ald} angle. There is also folding of the CH_3 group.[10] The magnitudes of these changes for 180° rotation are shown in Figure 1. To address the question What is the driving force behind these structural changes? we now construct alternate paths for conversion of the equilibrium (E) conformation to the staggered (S) conformation. Along these hypothetical paths the methyl group is rotated from eclipsed to staggered through the virtual conformation S* where the rest of the molecule variously remains partially frozen. The energetics for these processes are given in Table 4.

(20) (a) Ruedenberg, K. *Rev. Mod. Phys.* **1962**, *34*, 326. (b) Feinberg, M. J.; Ruedenberg, K.; Mehler, E. *Adv. Quantum Chem.* **1970**, *5*, 27.
(21) Feinberg, M. J.; Ruedenberg, K. *J. Chem. Phys.* **1971**, *54*, 1495.

Table 4. MP2/6-311G(3df,2p) Partitioned Energy Differences (Δ) for Different Paths, E ⇒ S* and S* ⇒ S (in cm^{-1})[a]

energy diff[b]	path I[c] S*(C−C)	path II[c] S*(∠CCO)	path III[c] S*(∠CCH_{ald})
Δ = (S*) − (E)			
ΔE	468	481	477
ΔT	−1454	1706	1605
ΔV	1922	−1224	−1228
ΔV_{nn}	−22874	17750	2878
ΔV_{ee}	−21253	19577	4816
ΔV_{ne}	46049	−38552	−8821
ΔV_r	−44127	37327	7694
Δ = (S) − (S*)			
ΔE	−30	−43	−40
ΔT	1278	−1882	−1781
ΔV	−1308	1838	1742
ΔV_{nn}	17052	−23572	−8700
ΔV_{ee}	17940	−22890	−8129
ΔV_{ne}	−36300	48301	18570
ΔV_r	34992	−46462	−16829

[a] S* represents a virtual state (see text), E the equilibrium eclipsed conformer, and S the fully relaxed staggered conformer. [b] See Table 2 footnote *a*. [c] S*(C−C) is the same as S[RF] except the C−C bond is allowed to lengthen to the C−C bond distance in S, S*(∠CCO) is the same as S[RF] except ∠CCO narrows to ∠CCO in S, S*(∠CCH_{ald}) is the same as S[RF] except ∠CCH_{ald} is allowed to widen to ∠CCH_{ald} in S.

Path I: E ⇒ S*[C−C]. C−C Bond Expansion. The C−C bond distance in S[RF] is lengthened to its ultimate length appropriate to S. The remaining skeleton, skeletal hydrogen, and methyl bond distances and angles remain fixed at the geometry of the eclipsed conformer. The important outcome is that a 0.007 Å expansion in the C−C bond length on rotating the methyl group to the staggered conformation causes the kinetic energy to strongly *decrease* and the potential energy to *increase*. The individual potential terms also undergo sign reversals from those found for rigid rotation (Table 4). *Hence the effect of C−C bond expansion is to change the sign of the internal rotation energy terms from those found for rigid rotation to those for the fully relaxed process.*

It is instructive to consider path I a two-step process: E ⇒ S[RF] ⇒ S*[C−C]. The electron repulsion, electron−nuclear attraction, and nuclear repulsion changes for the second S[RF] ⇒ S*[C−C] step overwhelm the changes found for the first rigid rotation step {i.e., E ⇒ S[RF]}. *Thus to give a cogent argument for the physics of the acetaldehyde barrier requires an understanding of the skeletal flexing that accompanies internal rotation.* To this end it is intriguing that the very small C−C bond length increase causes a large decrease in the electron repulsion energy.

Path II: E ⇒ S*[∠CCO]. CCO Angle Contraction. In order to obtain further insight into the barrier origin we now follow the rigid rotation step by CCO angular contraction to the value calculated for S. The signs of the energy terms resulting from this motion do not resemble the fully relaxed terms in Table 2. In fact, the overall effect is parallel to the rigid rotation step, E ⇒ S[RF], but larger.

Path III: E ⇒ S*[∠CCH]. CCH_{ald} Angle Expansion. For this path we keep the rigid frame S[RF] geometry with the exception that ∠CCH_{ald} is allowed to widen to ∠CCH_{ald} in S. Both signs and magnitudes of the individual terms resemble E ⇒ S[RF]. The close similarity to rigid rotation energetics infers that this relaxation plays only a small role in barrier energetics.

The overall conclusion obtained from consideration of energetics of the three paths is that only the C−C flexing path, S[RF] ⇒ S*[C−C] (path I), yields the same signs as the full internal rotation process, E ⇒ S. But the magnitudes of these energy changes are too large. The other flexing motions (e.g., paths II and III) compensate to reduce these large changes to magnitudes congruous to E ⇒ S. Hence they have opposite signs to the E ⇒ S energy terms. Thus partial undoing of the C−C bond plays a role in the acetaldehyde internal rotation barrier.

(b) According to Symmetry Type. At this point we now turn to an important subdivision of the overall energy partitioning discussed under (a). Acetaldehyde is predicted to retain its equilibrium conformation C_s symmetry on going to the top of the barrier (Figure 1), allowing the potential terms in Tables 2, 3, and 4 to be additionally broken down into contributions from a′ and a″ orbitals. Since the molecular skeleton remains planar and the methyl-group valence orbitals can be classified as π and σ types,[22] this symmetry partitioning naturally separates π and σ effects. The MP2 level results are given in Table 5 for E ⇒ S, E ⇒ S[RF], and E ⇒ S*[C−C].

We first focus on the kinetic energy terms. As described in the previous section T increases for E ⇒ S[RF] but decreases for E ⇒ S. An important clue to the link between energetics and electron distribution is provided by the individual (π and σ) ΔT terms: i.e. $T(\pi)$ always increases, whereas $T(\sigma)$ always decreases no matter what rotation process. The increase in $T(\pi)$ is quite understandable from the increased π-electron overlap in the staggered conformation over that in the eclipsed conformation. This increased overlap is basic to the π-fragment model for internal rotation and is discussed in the following section. The additional step S[RF] ⇒ S*[C−C] in the internal rotation process only introduces a small additional change in $T(\pi)$, inferring that π overlap does not change greatly for a 0.007 Å increase in C−C bond length.

In contrast to the positive π effect, the negative sign of $\Delta T(\sigma)$ implies an increase in the spatial extent of σ electrons. The largest decrease in $\Delta T(\sigma)$ is found for E ⇒ S*[C−C], i.e. path I. Path I introduces C−C bond expansion as sole alteration to the rigid rotation E ⇒ S[RF] process. The large decrease for the S[RF] ⇒ S*[C−C] step, $\Delta T(\sigma)$ = ca. -2600 cm^{-1}, leads to the conclusion that *C−C bond lengthening is an important source of the large $\Delta T(\sigma)$ decrease for the overall internal rotation process, E ⇒ S.*

Thus it becomes clear that the overall kinetic energy change is controlled by the $\Delta T(\sigma) + \Delta T(\pi)$ balance. For E ⇒ S[RF], $|\Delta T(\pi)| > |\Delta T(\sigma)|$, and the positive sign of ΔT(overall) is due to $\Delta T(\pi)$. But, for both E ⇒ S*[C−C] and E ⇒ S, ΔT(overall) < 0 is due to $|\Delta T(\sigma)| > |\Delta T(\pi)|$. The driving force always involves π electrons [$\Delta T(\pi)$ always >0] even for fully relaxed rotation where ΔT(overall) < 0. The important point is that the change in sign of ΔT(overall) in going from rigid to fully relaxed rotation results from the σ electron density changes engendered by C−C bond expansion.

We now turn to the much larger ΔV_{ne} term. Again starting with rigid rotation, E ⇒ S[RF], the π term $\Delta V_{ne}(\pi)$ decreases and this decrease overwhelms the opposite sense σ term, $\Delta V_{ne}(\sigma)$. But for E ⇒ S, although the signs of the changes remain the same, the magnitudes are in the opposite direction, i.e., $|\Delta V_{ne}(\pi)| < |\Delta V_{ne}(\sigma)|$. Thus, the σ term dominates both ΔT(total) and ΔV_{ne}(total) terms and consequently $\Delta E_{core} = \Delta T + \Delta V_{ne}$ for the fully relaxed process, E ⇒ S. *We conclude that it is the σ term that controls barrier energetics in actual internal rotation.* The confusion that exists about the π term arises because it is this term that is dominant in one-dimensional rigid-rotation models.

One explanation that has been offered for the large σ contribution ($\Delta V_{ne}(\sigma)$ = ca. $+35\,000$ cm^{-1}) to the barrier origin *for the process E ⇒ S[RF]* is breaking of a weak covalent bond

(22) Hoffman, R. *Pure Appl. Chem.* **1970**, *24*, 567.

Table 5. Partitioned Energy Differences (cm^{-1}) According to Symmetry

energy diff[a]	symmetry[b]	E ⟶ S[RF][c]	E ⟶ S*(C−C)[c]	E ⟶ S	S[RF][c] ⟶ S
kinetic energy (ΔT)	A′	−3240	−5878	−5026	−1786
	A″	4636	4424	4850	214
$\Delta T(\sigma+\pi)$	A′ + A″	1396	−1454	−176	−1572
electron-nuclear attraction energy (ΔV_{ne})	A′	38300	83504	58038	19738
	A″	−45840	−37455	−48290	−2450
$\Delta V_{ne}(\sigma+\pi)$	A′ + A″	−7540	46049	9748	17288

[a] See Table 2 footnote *a*. [b] A′ and A″ represent σ- and π-type charge distributions, respectively. [c] See Table 3 footnote *a* and Table 4 footnote *c*.

Table 6. Partitioned Energy Differences (kcal/mol) for Various Atomic Basins

		atom[b]			
energy diff[a,b]	path	C_1	C_2	O	H_{ald}
$\Delta T(\alpha)$	E ⟶ S[RF][c]	0.8	1.4	2.2	1.0
	E ⟶ S[c]	−3.4	0.2	3.4	−0.3
$\Delta V_{ne}(\alpha)$	E ⟶ S[RF][c]	13.5	−22.2	−25.2	−7.1
	E ⟶ S[c]	53.5	−12.1	−63.0	23.1

[a] See Table 2 footnote *a*. [b] α designates atomic basins; C_1 = carbonyl carbon, C_2 = methyl carbon. [c] See Table 3 footnote *a*.

between the carbonyl oxygen and the eclipsed methyl hydrogen, first suggested by Jorgensen and Allen.[23] Weak interaction between the oxygen nonbonding electrons and the eclipsed methyl hydrogen would be consistant with the calculated differential electron density map,[24] showing that the methyl in-plane hydrogen density increases, but decreases at the oxygen. An unambiguous requirement for such a bond is the presence of a bond critical point between the nuclei.[15,25] No such critical point was found in Wigerg and Martin's analysis of 6-31G(d) wave functions.[21] Our application of the more sensitive Cioslowski criterion[26] for weak bonds also yields a negative result. Further, there is an additional ~45 000 cm^{-1} increase in $V_{ne}(\sigma)$ for S[RF] ⟶ S*[C−C] (Table 5). Recalling that the sole difference between S[RF] and S*[C−C] is a 0.007 Å C−C bond lengthening, it seems unlikely that the large increase has much to do with methyl−oxygen bonding.

(c) According to Region. We now tie the symmetry partitioned energy terms discussed in the preceeding section to skeletal atomic basin energy terms given in Table 6. Because PROAIM implicitely makes use of kinetic energies to obtain local basin energies, these calculations were carried out at the virial theorem satisfying HF/6-31G(d,p) level. We start with rigid rotation, E ⟶ S[RF]. The largest atomic potential and kinetic energy contributions to E ⟶ S[RF] come from the methyl carbon atom (C_2) and oxygen, e.g., $\Delta E_{core}(\alpha) = -21$ kcal/mol for C_2, +14 for C_1, −23 for O, and −6 for the aldehyde hydrogen. Combining these results with the dominance of $\Delta V_{ne}(\pi)$ and $\Delta E_{core}(\pi)$ obtained from Table 5 suggests that in the rigid frame model the dominant potential terms arise from π-electron polarization toward the methyl-carbon atom,[27] as internal rotation proceeds.

But when the full torsional process E ⟶ S is considered, the largest core contributions come from the carbonyl carbon (C_1), $\Delta E_{core}(C_1) = 50$ kcal/mol vs $\Delta E_{core}(C_2) = -12$ kcal/mol, reflecting the large σ effect that is triggered by C−C expansion.

III. Nuclear Virial Energies. At this point we reconcile the difference in kinetic energy changes found for rigid and fully relaxed rotation. We start with the large kinetic energy increase found for rigid rotation, following BCLWB's lead in their study of the ethane rotational barrier to use the virial theorem as a basis for breaking up the total electronic energy. BCLWB obtained virials of the forces acting on the ethane nuclei as the methyl groups rotate through the general virial theorem

$$T = -E + \sum_{\alpha} \mathbf{X}_{\alpha} \cdot \mathbf{F}_{\alpha} \tag{3}$$

In eq 3 $\mathbf{X}_{\alpha} \cdot \mathbf{F}_{\alpha}$ is the contribution of the nucleus α to the virial of the forces acting on the electrons, $\mathbf{X}_{\alpha}$ is the position vector of α, and $\mathbf{F}_{\alpha} = -\nabla_{\alpha} E$ is the net force acting on it. When the forces acting on the nuclei vanish, as they do in the acetaldehyde equilibrium eclipsed conformation, the virial forces exerted on the electrons vanish and $T = -E$. When there are repulsive virial forces acting on the nuclei, as there will be in the acetaldehyde rigid-frame conformation, $T > |E|$.[28]

We now apply this idea to the nonequilibrium conformations, S[RF] and S*. Since we are taking differences between a state where the forces do not vanish and the equilibrium state, E, where they do, the difference represents only the nuclear virial for the nonequilibrium state. Thus for the torsional processes E ⟶ S[RF] and E ⟶ S*.

$$\Delta T = -\Delta E + \sum_{\alpha} \mathbf{X}_{\alpha} \cdot \mathbf{F}_{\alpha} \tag{4}$$

In particular, ΔT is positive and exceeds the magnitude of ΔE for E ⟶ S[RF] (see Table 3). Thus the potential energy change of the electrons is dominated by virial repulsive forces acting on the nuclei when the acetaldehyde skeleton is frozen during methyl torsion.

Equation 4 can be recast into the potential energy change, ΔV:

$$2\Delta E = \Delta V + \sum_{\alpha} \mathbf{X}_{\alpha} \cdot \mathbf{F}_{\alpha} \tag{5}$$

As discussed earlier, the overall change in potential energy is negative for rigid rotation, i.e., the attractive contributions dominate. (We emphasize that this change is opposite to that for the overall process E ⟶ S.) From Table 3, $V_a + V_r < 0$, *therefore a rigid rotation description of torsion in acetaldehyde leads to a barrier which does not arise from potential energy contributions, but from the virials of repulsive forces acting on the nuclei in the nonequilibrium geometry.*

This conclusion is parallel to one drawn by BCLWB for internal rotation in ethane. In contrast, on going to the virtual state S*[C−C], ΔT is negative, i.e., there is no repulsive nuclear virial for the partially relaxed path I (see Table 4) where only the C−C bond is allowed to expand, all other coordinates

(23) Jorgensen, W. L.; Allen, L. C. *J. Am. Chem. Soc.* **1971**, *93*, 567.
(24) Wiberg, K. B.; Martin, E. *J. Am. Chem. Soc.* **1985**, *107*, 5035.
(25) Bader, R. F. W.; Tal, Y.; Anderson, S. G.; Nguyen-Dang, T. T. *Isr. J. Chem.* **1980**, *19*, 8.
(26) Cioslowski, J.; Mixon, T. *J. Am. Chem. Soc.* **1993**, *115*, 1084.
(27) Baba, M.; Nagashima, U.; Hanazaki, I. *J. Chem. Phys.* **1985**, *83*, 3514.

(28) See Section IIa for comments on MP2 $|\Delta T|$, $|\Delta E|$ discrepancies, where $|\Delta T| < |\Delta E|$ at the equilibrium position.

remaining frozen. Further the overall potential energy change is now positive. The implication is that the torsional barrier for rigid rotation arises from virials of repulsive forces *acting on the carbon−carbon bond.* This is also evident from the atomic contributions to the process E ⇒ S[RF], which come primarily from the carbon atoms, $\Delta T(C_1) + \Delta T(C_2) = 2.2$ kcal/mol; $\Delta V_a(C_1) + \Delta V_a(C_2) = -8.7$ kcal/mol (Table 6). Final confirmation is provided by the parallel outcome of rigid rotation to paths II and III, i.e., only expansion of the C−C bond removes the repulsive nuclear virial.

Conclusions

Our leading conclusion is that *the origin of the changes in attractive and repulsive energies occurring during internal rotation cannot be understood without appreciation of the role that skeletal flexing plays in controlling the energetics.* If the skeleton is frozen at the eclipsed equilibrium geometry during methyl rotation, opposite potential and kinetic energy changes to the fully relaxed (multidimensional) adiabatic torsional process take place. Under this one-dimensional rigid rotation the barrier does not arise from potential energy terms since the sum of these terms is antibarrier. It actually arises from nuclear virial contributions to the kinetic energy.

There is a second major conclusion, derived from partitioning of the barrier energetics into σ and π terms for multidimensional fully relaxed rotation. The σ-electron nuclear−electron attraction energy increases counter to that for the π electrons. *The principal source of the σ increase is lengthening of the C−C bond accompanying methyl torsional motion.* A similar conclusion is obtained for an internal rotation model which only includes C−C flexing. But for the rigid rotation the kinetic energy barrier forming term is due to the π electrons. *It would seem that the π-fragment model for internal rotation energetics in acetaldehyde has as its basis a one-dimensional rigid-frame description of methyl rotation.*

Overall ΔT and ΔV values by themselves are insufficient to unambiguously identify the driving force for the barrier origin; however the energy changes that we have documented here must be taken into account in any future explanation of the barriers, e.g. what changes in σ electron density cause weakening of the C−C bond? Small changes (at the 10^{-2} level) in Cioslowski bond orders[29] are found.[30] However, substantial changes in the in-plane components of the atomic quadrupole moment tensor for the carbonyl carbon[31] suggest another possibility, asymmetry in the C−C region charge distribution.

In summary we conclude that the origin of the acetaldehyde internal rotation barrier is complex. For methyl rigid rotation the nuclear virial repulsive energy contribution to the kinetic energy change arises from the π electrons. To remove the positive nuclear virial, the molecule has to relax by C−C bond lengthening. This lengthening causes both σ and π core energies to increase. But the greater sensitivity of the former to C−C bond lengthening overwhelms the π contribution. In the stretched C−C bond conformation it is σ electrons which lead to correct barrier energetics. Other flexings correct the magnitude of individual energy terms but do not change any conclusions. Because of this great sensitivity of σ and π interactions to skeletal relaxation, models for the physical origin of the barrier which do not take into account the multidimensional nature of internal rotation (such as the π-fragment model) are suspect and do not allow intuition. While we have only proved this result for ground state acetaldehyde, the analysis has a wider reach and applies to other states, both neutral and ionic, of acetaldehyde and to other conjugated molecules.

Acknowledgment. We thank the donors of the Petroleum Research Fund, administered by the American Chemical Society, for the Visiting Faculty Fellowship and the National Science Foundation for financial support and also the Pittsburgh Supercomputer Center for a computational grant. We are grateful to Prof. Jerzy Cioslowski for critically reading the manuscript, Dr. Paul Rablen (Yale University) for many helpful conversations, and John Westbrook (Rutgers Chemistry Department High Performance Computation Project) for aid with the modification of GAUSSIAN 92.

JA942233U

(29) Cioslowski, J.; Mixon, T. *J. Am. Chem. Soc.* **1992**, *114*, 4382.
(30) Unpublished calculations of the authors.
(31) MP2/6-311G(3df,2p) $\Delta Q_{xx} = 0.89$, $\Delta Q_{xz} = -0.67$ where the x is in-plane perpendicular to the C−C bond axis (z).